Inorganic Chemistry

Article

pubs.acs.org/IC

N,N′-Fused Bisphosphole: Heteroaromatic Molecule with Two-Coordinate and Formally Divalent Phosphorus. Synthesis, Electronic Structure, and Chemical Properties

Alexander N. Kornev,*[,†] Vyacheslav V. Sushev,[†] Yulia S. Panova,[†] Olga V. Lukoyanova,[†] Sergey Yu. Ketkov,[†] Evgenii V. Baranov,[†] Georgy K. Fukin,[†] Mikhail A. Lopatin,[†] Yulia G. Budnikova,[‡] and Gleb A. Abakumov[†,§]

[†]G. A. Razuvaev Institute of Organometallic Chemistry, Russian Academy of Sciences, 49 Tropinin str, 603950 Nizhny Novgorod, Russia

[‡]A. E. Arbuzov Institute of Organic and Physical Chemistry, Kazan Scientific Center of Russian Academy of Sciences, 8 Arbuzov str, 420088 Kazan, Russia

[§]Chemical Department, Lobachevsky State University of Nizhny Novgorod, 23 Gagarina Pr, 603950 Nizhny Novgorod, Russia

Supporting Information

ABSTRACT: The reduction of 6,12-dichloro-1,2,3,4,7,8,9,10-octahydro-6*H*,12*H*-[1,2,3]benzodiazaphospholo[2,1-*a*][1,2,3]-benzodiazaphosphole (**3**) by metallic magnesium in tetrahydrofuran (THF) affords the N,N′-fused bisphosphole **1** in 92% yield. The compound reveals a novel type of 10π-electron heteroaromatic system [NICS(0) = −11.4], containing a two-coordinate and formally divalent phosphorus atom. Compound **1** possesses a much higher coordination activity than many other diazaphospholes. This is caused by a novel type of complexation to a metal ion wherein the lone phosphorus pairs are not involved in metal coordination. Instead, the 10π-electron heteroaromatic system provides two electrons for P → M bond formation. Polarization of the ligand results in the formation of extended molecular associates or cluster compounds. Complexes of **1** with mercury dichloride [{(**1**)$_3$HgCl}$_2$(μ_6-Cl)]$^+$Cl$^-$ (**7**) and tin dichlorides [**1**·SnCl$_2$(PhMe solvate)] (**8a**) and [**1**·SnCl$_2$] (**8b**) are, in fact, supramolecular in nature, containing multiple intermolecular short contacts. Crystals of complex **8a** containing short Sn···Sn packing interactions were converted reversibly to metallic tin after workup with THF. The simple mixing of **1** and **3** (1:1) gave a P−P bridging dimeric species prone to easy dissociation. The addition of GeCl$_2$(diox) to the equimolar mixture of **1** and **3** shifted the equilibrium to the formation of a poorly soluble salt-like dimer **6**, which is, in fact, a stacked 18π-electron dication having a through-space delocalization of π electrons.

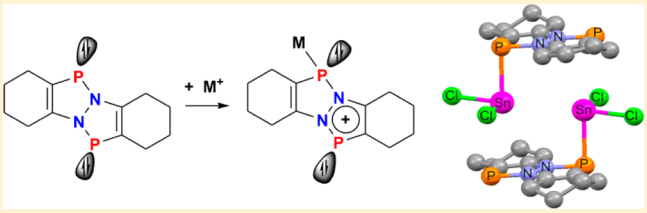

INTRODUCTION

Phospholes are key building blocks for the engineering of conjugated polymers.[1] A variety of linear and cyclic oligomers as well as polymeric derivatives incorporating phospholes have been synthesized.[2] Apart from conductive polymers, phosphole-containing building blocks have also been used for the tailoring of nonlinear-optical (NLO) phores and emissive materials for organic light-emitting devices (OLEDs).[2,3] Azaphospholes, which have been the subject of a number of articles and reviews,[4−6] are five-membered 6π aromatic phosphorus heterocycles having a σ^2,λ^3-phosphorus atom and a σ^3,λ^3-nitrogen atom as ring members. The two-coordinate phosphorus contributes one π electron to the aromatic sextet, but the donation of two π electrons by a nitrogen atom furnishes a neutral five-membered system (Chart 1).

The majority of azaphospholes are as stable and unreactive as the familiar classical aromatic five-membered heterocycles. The most interesting reactions of azaphospholes are the 1,2-addition to their C═P or N═P double bonds (the addition of protic reagents, [2 + 4]cycloaddition).[5a] There are, however, considerable and characteristic differences in reactivity even among the isomers of the same ring system. Among diazaphospholes, dihydro-1,3,2-diazaphospholes are perhaps

Chart 1

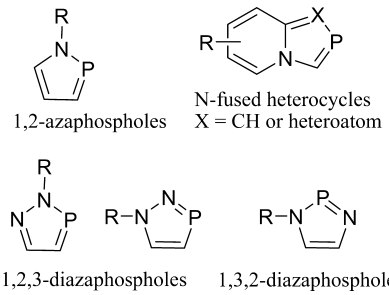

Received: February 4, 2014
Published: February 21, 2014

   dx.doi.org/10.1021/ic500274h | Inorg. Chem. 2014, 53, 3243−3252

the most thoroughly investigated precursors of phosphorus analogues of Arduengo carbenes.[5c−e] The chemistry of related 1,2,3-diazaphospholes has been extensively studied by Schmidpeter, Bansal and Heinicke, and others.[4a,5e] It is also worth noting that there is a large class of N-fused heterocycles in which a planar nitrogen atom contributes two π electrons to the aromatic system (Chart 1).[4,5,7−11]

We now report a novel type of annulated heterophosphole **1** (Chart 2), based on a planar hydrazine block. This compound,

Chart 2. Graphical Representations of 1 and 2[a]

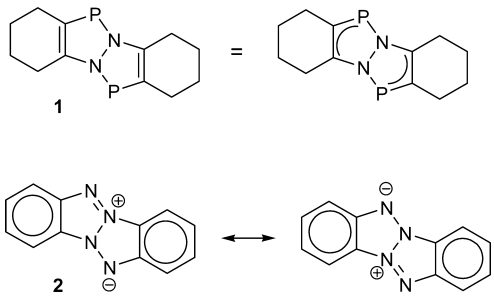

[a]For B3LYP/6-31G(d) Mulliken charges in **2**, see Figure S1 in the SI.

being a relative of the above-mentioned types of azaphospholes, nevertheless, displays quite untypical chemical properties. The curious feature of this hydrazine-fused bisphosphole is in its unusual chemical structure, which is impossible to depict by classical Lewis schemes. Compound **1** is an analogue of tetraazapentalene (**2**).[12] However, it would be incorrect to consider **1** as a mesoionic compound like **2** because phosphorus atoms are less electronegative than the adjacent nitrogen atoms and the molecule has centrosymmetric geometry.

Such Lewis-type structures are oversimplifications of the actual bonding. More accurate models of the actual electronic structures of such molecules are obtained from computational investigations or inferred from structural and reactivity studies. Although nitrogen−phosphorus compounds exhibit greater structural diversity, including a wide range of coordination numbers, the limits of the structure and bonding for nitrogen−phosphorus compounds have not yet been realized. The synthesis and structure of the unusual bisphosphole **1** and its reactions with metal halides ($HgCl_2$, $SnCl_2$, and $GeCl_2$) are presented below.

RESULTS AND DISCUSSION

Synthesis, Spectroscopic, and Structural Characterization of 1 and 3. The N,N′-fused bisphosphole **1** was prepared from the reduction of 6,12-dichloro-1,2,3,4,7,8,9,10-octahydro-6*H*,12*H*-[1,2,3]benzodiazaphospholo[2,1-*a*][1,2,3]-benzodiazaphosphole (**3**)[13] with magnesium in a tetrahydrofuran (THF) solution (eq 1).

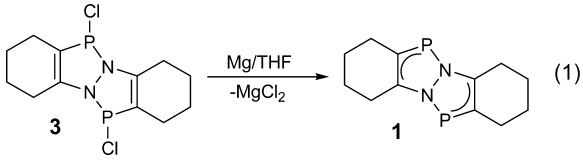

(1)

The vigorous reaction gives a clean orange solution without precipitation of magnesium chloride. The orange crystalline **1** was separated from $MgCl_2$ by recrystallization from a hexane solution and further sublimation at 110 °C/0.01 mmHg. The reduction of **3** was also observed with other alkaline- and rare-earth metals (Na/Hg, KC_8, Ca, Gd, and Eu). In these cases, however, it was difficult to achieve complete reaction and/or obtain a pure product. It should be mentioned that the reduction of a compound structurally related to **3** (namely, 4,8-di-*tert*-butyl-2,6-dichloro-1,5-diaza-2,6-diphosphabicyclo[3.3.0]-octa-3,7-diene) with a Na/K alloy caused splitting of the diazaphosphole cycle and unexpectedly gave a substituted cyclohexaphosphane.[14]

The room-temperature ^{31}P NMR spectrum of diamagnetic **1** has a single absorption at 177.0 ppm. This value is strongly shifted upfield compared to the resonances usually observed for azaphospholes (200−240 ppm).[4,5] The ^{13}C NMR spectrum shows a double resonance at 142.8 ppm ($^1J_{C,P}$ = 48 Hz) and multiple resonances at 128.6 ppm corresponding to the sp^2 carbon atoms (*C*P and *C*N respectively; Figure S2 in the Supporting Information, SI) and overlapping multiplets in the region of 21−25 ppm from four nonequivalent CH_2 groups. The IR spectrum of **1** reveals a similarity with the spectrum of the starting dichloro derivative **3** with the exception of the absorption bands P−Cl (480 and 466 cm^{-1}), which are absent in **1**.

The structure of **1** was determined by X-ray analysis (Figure 1). Crystal data and some details of the data collection and

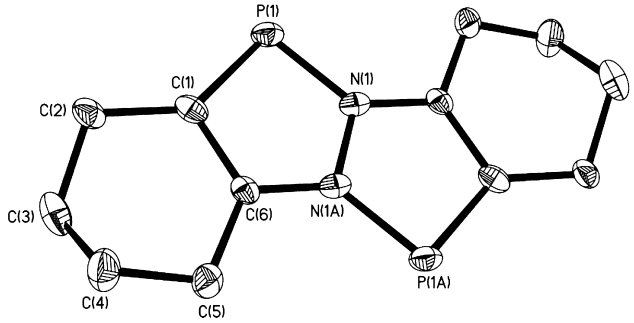

Figure 1. Molecular structure of **1**. Ellipsoids are drawn at 30% probability. Hydrogen atoms of *c*-hexenyl rings are omitted for clarity. Selected bond distances (Å) and angles (deg) for **1**: P(1)−N(1) 1.733(5), P(1)−C(1) 1.755(5), N(1)−N(1A) 1.368(11), N(1)−C(6A) 1.373(8), C(1)−C(6) 1.335(7), C(1)−C(2) 1.529(6), C(2)−C(3) 1.545(6), C(6)−N(1A) 1.373(8); N(1)−P(1)−C(1) 88.8(3), N(1A)−N(1)−C(6A) 108.8(6), N(1A)−N(1)−P(1) 114.4(5), C(6A)−N(1)−P(1) 136.7(4), C(6)−C(1)−P(1) 110.0(4), C(2)−C(1)−P(1) 130.7(4), C(1)−C(6)−N(1A) 117.9(5), C(1)−C(6)−C(5) 128.9(5), N(1A)−C(6)−C(5) 113.2(5).

refinement are given in Table S1 in the SI. The centrosymmetric structure of **1** is characterized by the presence of planar geometry of the diazaphosphole rings. In the crystal, the whole molecule of **1** is disordered over two special positions about the inversion center of the lattice (Figure S3 in the SI). The site occupancy factors are approximately equal. Two disordered parts of **1**, labeled as **1a** and **1b**, have close geometry (Table S2 in the SI). Therefore, the structure of **1** will be considered with only one disordered part, **1a**. The bond distance between the two carbon atoms in the PCCN fragment [1.335(7) Å] corresponds to the normal double C═C bond in alkenes. The C−P, P−N, N−N, and N−C bond lengths lie in the range typical of 1,2,3-diazaphospholes.[5,15] It is important to note that the shortest distances between the phosphorus atoms of

dx.doi.org/10.1021/ic500274h | Inorg. Chem. 2014, 53, 3243−3252

adjacent molecules in the crystal (4.180 Å) exceed the sum of the van der Waals radii (3.60 Å).[16]

The electrochemical reduction of **3** is characterized by two stages (Figure 2). The first two-electron irreversible wave of

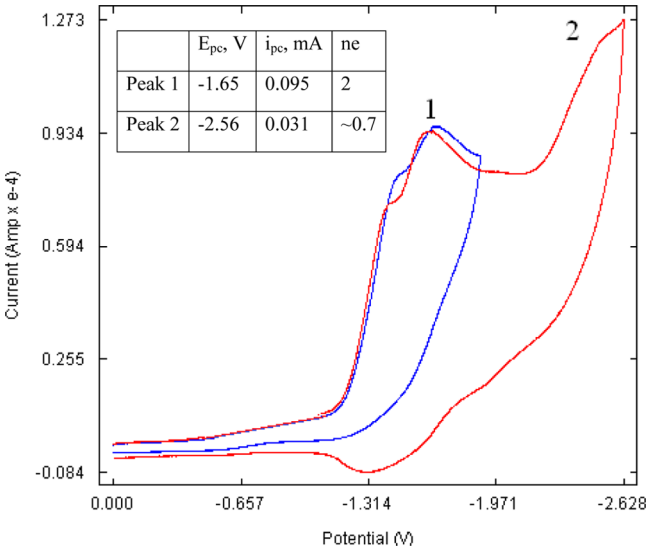

Figure 2. Cyclic voltammograms of **3**. DMF, $C = 5 \times 10^{-3}$ M. The reference electrode is SCE. The working electrode is glassy carbon. The background salt is Et_4NBF_4.

complex shape at −1.65 V is observed, resulting from a superposition of two peaks at similar potentials related to the reduction of two nonequivalent P−Cl bonds. The next stage is characterized by a quasi-reversible peak at −2.56 V, or more precisely, by a cathodic peak with an associated anodic oxidation peak but with a rather large difference between the potentials of direct and reverse peaks (about 1.2 V). The reduction of **3** can be represented as follows (eq 2).

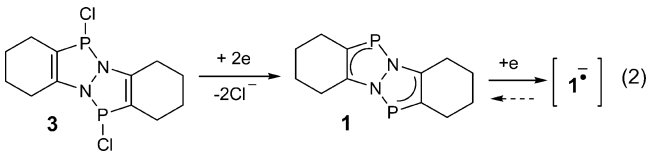

We did not succeed in fixing the anion radical of **1** by electron paramagnetic resonance apparently because of its high reactivity. On the other hand, in the course of preparative electrolysis of **3**, along with the formation of **1** (registered by ^{31}P NMR), an appreciable amount of the substance is polymerized at the cathode surface to give an insoluble black film.

Density Functional Theory (DFT) Calculations. In order to elucidate the nature of the bonding and to understand whether the NNPCC rings of **1** are aromatic, we performed DFT structural optimizations and frequency calculations at the B3LYP/6-31G(d) level of theory.[17] The calculated and experimental structures of **1** are generally in good agreement. The lowest-energy structure of **1** was found to be singlet electronic states displaying planar geometry of the nitrogen atoms and the diazaphosphole rings.[18] It should be noted, however, that the calculated C−P, P−N, and C═C bond lengths are slightly longer (by 2−3 pm) than those found experimentally (Figure S4 and Table S2 in the SI).

Evaluation of the molecular orbitals (MOs) of **1** reveals important contributors to the bonding between the phosphorus and adjacent atoms. Figure 3 displays the lowest unoccupied molecular orbital (LUMO) and the three highest occupied molecular orbitals (HOMOs) for **1**. The LUMO is a π^* orbital, localized on both diazaphosphole rings. The three HOMOs of **1** are mainly localized on the annulated heterocycles. The HOMO and HOMO−1 are essentially phosphorus p orbitals interacting with π electrons of the double C−C bond. It is remarkable that the nitrogen atomic orbitals do not contribute to the HOMO. The next occupied molecular orbital (HOMO−2) represents a π-conjugative interaction between the P−N and C═C bonds. The electronic spectrum of **1** in toluene (Figure 4) had a strong narrow absorption at 438 nm, which is close to the calculated HOMO−LUMO gap of 3.2 eV.

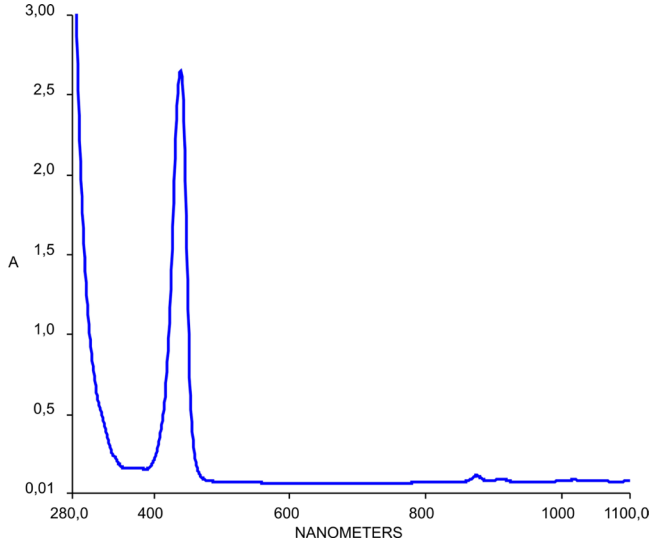

Figure 4. Electronic spectrum of **1** in toluene.

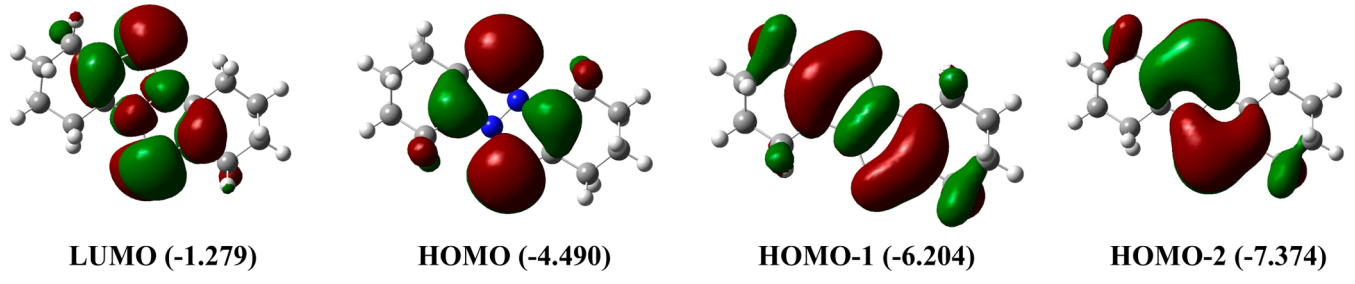

Figure 3. MOs for **1** and their energies in electronvolts.

dx.doi.org/10.1021/ic500274h | Inorg. Chem. 2014, 53, 3243−3252

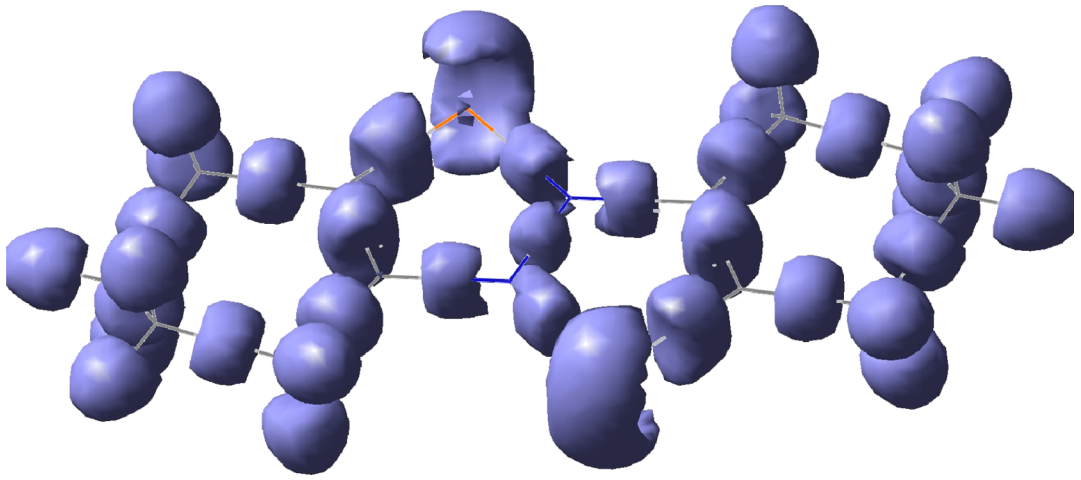

Figure 5. Visualization of the electron density of the lone pairs and bonding electrons in **1**.

Natural bond orbital (NBO) analysis of the optimized structure **1** shows a significant charge separation in the five-membered cycles: the nitrogen atoms bear partially negative charges (−0.394), while the phosphorus atoms are positively charged (+0.592); the carbon atoms, bonded to nitrogen and phosphorus, have partial charges of +0.141 and −0.422, respectively (Figure S5 in the SI).

The electron-pair localization regions were analyzed by the localized orbital locator function with the *Multiwfn 2.01* program.[19] Analysis showed that the electron density of the lone pairs possesses a mirror symmetry with respect to the plane of heterocycles (Figures 5 and 6).

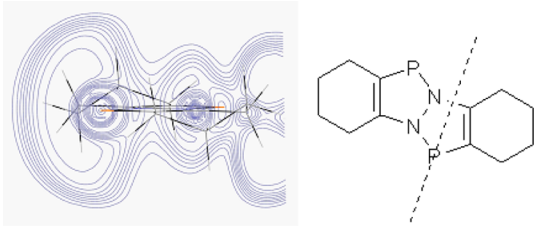

Figure 6. Contour electron density map for complex **1** calculated in the plane orthogonal to the plane of a C_2N_2P heterocycle.

The P−C and P−N bonds are characterized by high values of the ellipticity parameter calculated within the AIM theory[20] (0.46 and 0.31, respectively; Table 1). This is indicative of a large π contribution to bond formation. The ellipticity of N−N and N−C bonds increases slightly, while the values of the electron density remain quite high. So, all bonds in the five-membered cycles to some extent participate in the conjugation.

Table 1. Ellipticity $\lambda_1/\lambda_2 - 1$ and Electron Density (ρ) at the Bond Critical Points for Selected Bonds in Compounds 1 and 3

	$\lambda_1/\lambda_2 - 1$ (ρ)	
chemical bond	compound **3**	compound **1**
P−C	0.13 (0.154)	**0.46** (0.167)
P−N	0.09 (0.142)	**0.31** (0.135)
C−C	0.33 (0.351)	0.31 (0.320)
N−N	0.16 (0.316)	0.18 (0.352)
N−C	0.16 (0.312)	0.20 (0.301)
P−Cl	0.07 (0.087)	

Finally, we calculated the nucleus-independent chemical shift (NICS[21]) values for the five-membered rings of **1** to assess the aromatic character. Note that negative NICS values measure the magnitude of the aromaticity, while positive NICS values correspond to antiaromatic systems. Nonaromatic rings have NICS values close to zero. The theoretical data of NICS(0) = −11.44 and NICS(1) = −9.25 are indeed compatible with the aromatic character of the cyclic C_2N_2P moieties.

Interestingly, five-membered rings of dichloro derivative **3** reveal weak aromatic character, NICS(0) = −5.68. Although Huckel's $4n + 2$ rule is strictly intended for monocyclic systems, this rule may also be applied in certain cases to the π-bonded periphery of polycyclic molecules. Examples of such aromaticity are numerous; a good case in point is also 3a,6a-diazapentalene.[22] It is a bicyclic 10π-electron system. At the same time, the parent 8π-electron pentalene has by far eluded all synthetic efforts. The aromaticity of phosphorus heterocycles has been the subject of systematic and thorough investigations for the past decade.[23] A relation may also be found between **1** and unusual heterocyclic compounds containing four-membered planar rings (C−P−Si−P and Si−P−Si−P) with two-coordinate phosphorus atoms.[24] DFT calculations showed considerable electron delocalization over four-membered rings and negative NICS(0) and NICS(1) values.

Solution Behavior of 1 and 3. While **1** and **3** demonstrate quite ordinary spectral properties (NMR and electronic spectra), their equimolar mixture shows no ^{31}P NMR signal in THF or CH_2Cl_2 solutions at temperatures ranging from −50 to +50 °C. Meanwhile, the mixture reveals thermochromic and solvatochromic properties. The electronic spectrum of the mixture (1:1) in THF had a new absorption band at 525 nm, which rises in intensity with a decrease in temperature. Subtracting the spectrum measured at 20 °C from the spectrum measured at −100 °C results in the curve shown in Figure 7. The absorption band found with λ_{max} at 525 nm is in good agreement with the calculated energy (2.38 eV) of the electron transition from the HOMO of **1** to the LUMO of **3**. It is noteworthy that solvent removal from the mixture in a vacuum gave a dark-violet thin film showing a new very broad absorption band in the range of 800−1100 nm (Figure 8). These results conform to the concentration-dependent

dx.doi.org/10.1021/ic500274h | *Inorg. Chem.* 2014, 53, 3243−3252

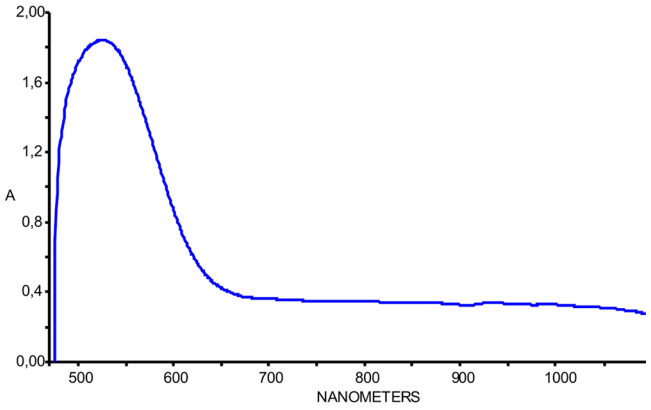

Figure 7. Resulting curve obtained by subtraction of the spectrum of the equimolar mixture **1** + **3** measured at 20 °C from the spectrum measured at −100 °C in THF.

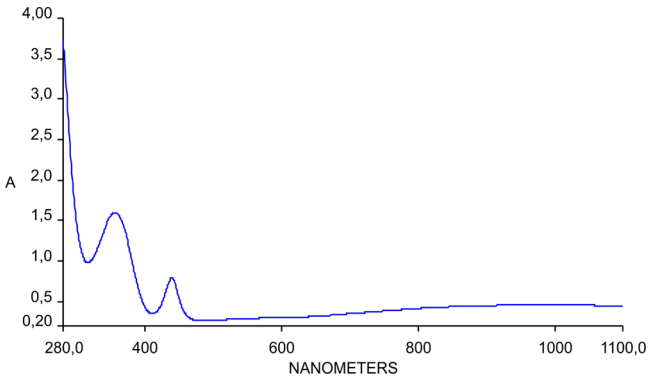

Figure 8. Electronic spectrum of the equimolar mixture **1** + **3** in thin film.

associations of **1** and **3** in the solution. In the cooled dilute solution, the pairs interaction of **1** and **3** is mainly observed, giving the absorption band at 525 nm. The concentrated solutions and thin film apparently contain extended conjugated associates of different length.

Two different structures for the primary association of **1** and **3** may be proposed. One of them is a chlorine-bridged dimer, **4**, and the other is a dimer containing a P−P bond, **5** (eq 3).

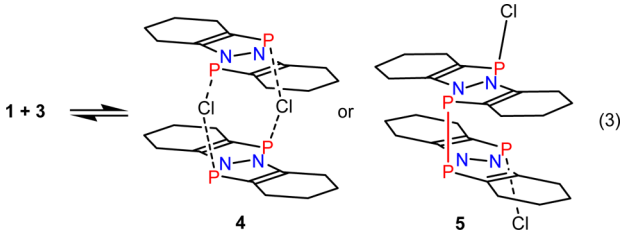

We succeeded in confirming that dimers like **5** are formed in this system. The addition of germanium dichloride to the equimolar mixture of **1** and **3** shifted the equilibrium entirely toward a poorly soluble salt-like dimer, **6** (eq 4).

The reaction proceeds in THF almost quantitatively to form a light-brown crystalline precipitate of **6**. The molecular structure of **6** is shown in Figure 9 with selected bond lengths and angles. Crystal data and some details of the data collection and refinement are given in Table S1 in the SI. Complex **6** contains an organophosphorus dication and two $GeCl_3^-$ anions, which take independent positions in the unit cell. The two

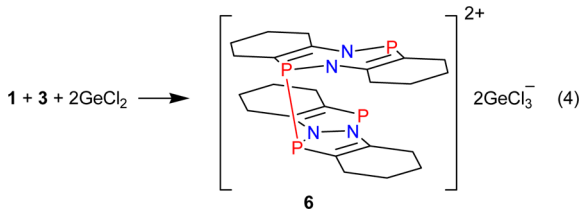

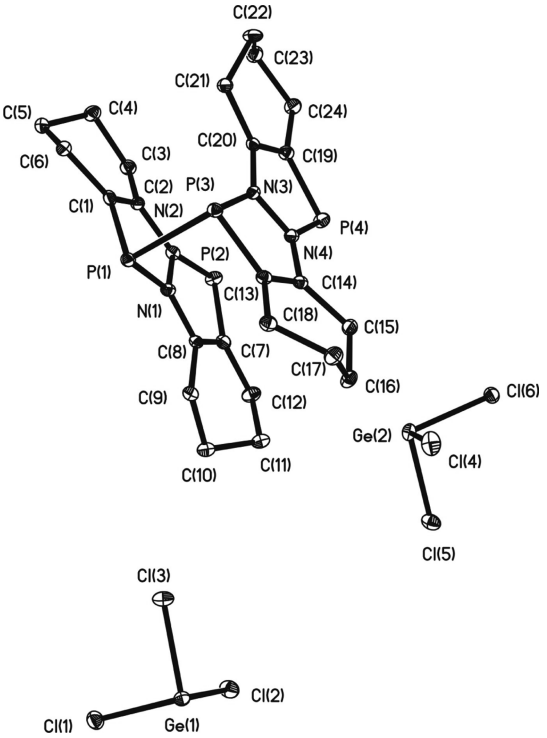

Figure 9. Molecular structure of **6**. Ellipsoids are drawn at 30% probability. Hydrogen atoms of *c*-hexenyl rings are omitted for clarity. Selected bond distances (Å) and angles (deg) for **6**: P(1)−N(1) 1.744(2), P(1)−C(1) 1.797(3), P(1)−P(3) 2.424(1), P(2)···P(4) 3.162(1), P(2)−N(2) 1.693(2), P(2)−C(7) 1.749(3), N(1)−C(8) 1.361(3), N(1)−N(2) 1.376(3), N(2)−C(2) 1.405(3), C(1)−C(2) 1.346(4), C(7)−C(8) 1.373(4), Ge(1)−Cl(2) 2.2811(7) (min), Ge(1)−Cl(3) 2.3187(7) (max); Cl(2)−Ge(1)−Cl(1) 94.69(3) (min), Cl(4)−Ge(2)−Cl(6) 97.32(3) (max), N(1)−P(1)−C(1) 87.8(1), N(1)−P(1)−P(3) 97.31(8), C(1)−P(1)−P(3) 96.56(9), N(2)−P(2)−C(7) 89.0(1), C(13)−P(3)−P(1) 97.67(9), C(8)−N(1)−N(2) 111.6(2), C(8)−N(1)−P(1) 134.1(2), N(2)−N(1)−P(1) 114.3(2), N(1)−N(2)−C(2) 110.6(2), N(1)−N(2)−P(2) 114.3(2), C(2)−N(2)−P(2) 134.9(2), C(2)−C(1)−P(1) 111.8(2), C(1)−C(2)−N(2) 114.7(2), N(2)−C(2)−C(3) 118.1(2), C(8)−C(7)−P(2) 111.7(2), N(1)−C(8)−C(7) 113.3(2).

bisphosphole units in the dication are linked by the P(1)−P(3) bond [2.424(1) Å], which is by some 21 pm longer than a standard single bond (2.214 ± 0.022 Å).[25] Interestingly, the distance between the other phosphorus atoms P(2)···P(4) [3.162(1) Å] does not exceed the sum of the van der Waals radii (3.60 Å).[16]

There is little difference in the bond distances and angles within **1** and **6**. Note, however, that five-membered heterocycles in the dication are rather nonplanar. The mean deviations of the atoms from the mean planes PC_2N_2 in the σ^3,λ^3-phosphorus heterocycles are 0.035 and 0.033 Å. The analogous values for heterocycles containing σ^2,λ^3-phosphorus are considerably lower (0.013 and 0.016 Å). This is in

dx.doi.org/10.1021/ic500274h | Inorg. Chem. 2014, 53, 3243−3252

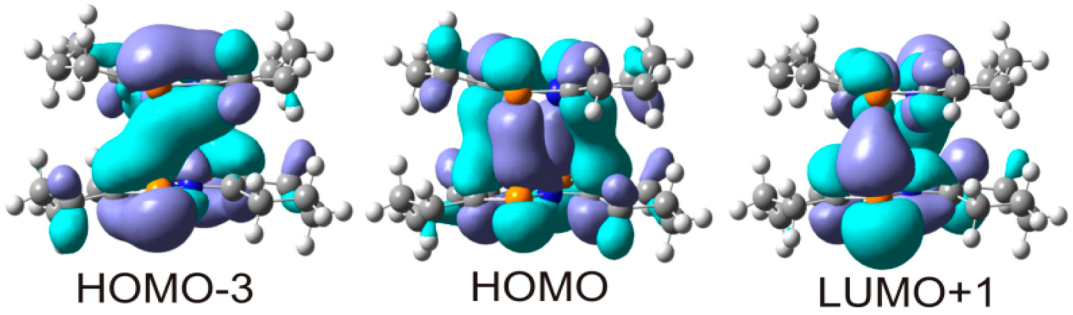

Figure 10. MOs for **6** (dicationic fragment).

agreement with the more aromatic character of heterocycles having two-coordinate trivalent phosphorus. NICS values confirm this observation. So, NICS(0) calculated for a σ^2,λ^3-phosphorus heterocycle is −14.9, while NICS(0) for a σ^3,λ^3-phosphorus heterocycle is −11.5. It is worth noting that NICS values for the latter increase gradually while going toward the adjacent bisphosphole unit and diminish toward the open side (Table S3 in the SI). Single-point calculations at the B3LYP/6-31G(d) level performed for the dication of **6** reveal that the frontier orbitals are localized mainly on the heterocycles (Figure 10). It is important to highlight that the bisphosphole units can effectively bind to each other not only by the P−P single bond but also by formation of the united π system, as shown in the shapes of the HOMO, HOMO−3, and LUMO+1 orbitals. Taking into consideration the steric factors, it may be supposed that the arrangement of the two positively charged bisphosphole units would be most favorable in the anti position relative to each other. Formation of the stacked 18π-electron dication may be explained by the concept of stacked-ring aromaticity assuming through-space delocalization of π electrons.[26] Considering the molecular structure of **6**, the particularly short P(2)···P(4) distance, and quite long P(1)−P(3) bond, it may be supposed that there is equilibrium in the solutions, which assumes simultaneous shortening of the P(2)···P(4) distance and lengthening of the P(1)−P(3) bond (eq 5):

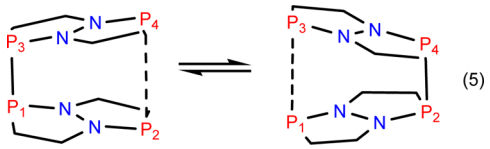

(5)

Such flexibility of bisphosphole units may be the reason for failures in ^{31}P NMR monitoring of the solutions containing **6** or a **1** + **3** equimolar mixture in polar solvents (THF and CH_2Cl_2). It was surprising when the dilute toluene solution of a **1** + **3** equimolar mixture gave good resolved ^{31}P NMR signals only after 1 week of being kept in a sealed tube. The two singlets at 104.6 and 103.1 ppm recorded at 223 K may be assigned to the phosphorus atoms belonging to the P−Cl and/or P−P fragments tentatively. The small difference (1.5 ppm) between the two resonances confirms the similarity of the electronic and structural parameters of the two nonequivalent phosphorus atoms in **5**. Both resonances disappeared again as a result of changing (increasing) the concentration of the solution apparently because of the formation of supramolecular associates.

N,N′-Fused Bisphosphole as a Ligand in Coordination Chemistry. It is known that aromatic azaphospholes are poor σ donors because a lone pair of the sp^2 phosphorus atom exhibits a higher degree of s character and is thus more diffuse and less directional.[5,27] The activity of N,N′-fused bisphosphole **1** in the coordination bond formation is much higher, which can be explained most likely by a different mechanism of complexation. While the lone pair of sp^2 phosphorus is poorly available, the 10π-electron system may submit another two electrons via the phosphorus atom, taking away one electron from the neighboring phosphorus (eq 6).

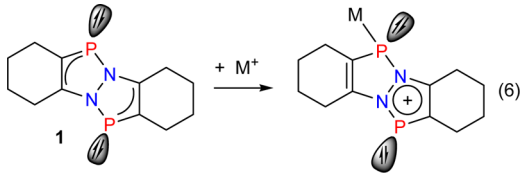

(6)

We succeeded in characterizing complexes of **1** with mercury(II) and tin(II) chlorides, which exhibit unique molecular and crystal structure. Mercuric chloride reacts with excess **1** to form a complex compound, $[\{(\mathbf{1})_3HgCl\}_2(\mu_6\text{-}Cl)]^+Cl^-$ (**7**; Figure 11). Note, however, that the reaction is accompanied by a partial mercury precipitation. The deep-red color of **7** can be explained by the strong polarization of the ligand. Both mercury atoms in **7** are tetrahedrally surrounded by a covalently bound chlorine atom and three diazaphosphole ligands coordinated by one phosphorus atom. The diazaphosphole ligands are arranged in such a way that the HgCl units are placed in a "container" of these ligands. Two cationic fragments $\{(\mathbf{1})_3HgCl\}^+$ are retained together by the chloride anion Cl(2), which is associated with the six phosphorus atoms simultaneously. The equal P−Cl(2) distances (3.58 Å) are close to the sum of the van der Waals radii (3.60 Å). Yet, one chloride ion is localized in the nodes of the crystal lattice. The diazaphosphole rings of both species were arranged with an all-gauche conformation along the Cl−Hg···Cl···Hg−Cl backbone, as depicted in Figure 11b,c, so that the phosphorus lone pairs were not directed toward the central chloride ion. The P−Hg bonds are quite long (2.560 Å) but do not exceed the sum of the van der Waals radii of the elements (3.35 Å).[16] The angle in between the N(1)−P(1)−C(1) plane and the P → Hg coordination bond is 104.64°. Coordination by mercury causes certain structural changes in the annulated heterocycles. The cycle bonded to the mercury atom reveals elongation of all chemical bonds relative to the free ligand. At the same time, the neighboring heterocycle exhibits contraction of the C−N, P−N, and C−P bond lengths, while the double C−C bond approaches those found in aromatic compounds (for comparison, see Table S4 in the SI).

dx.doi.org/10.1021/ic500274h | Inorg. Chem. 2014, 53, 3243−3252

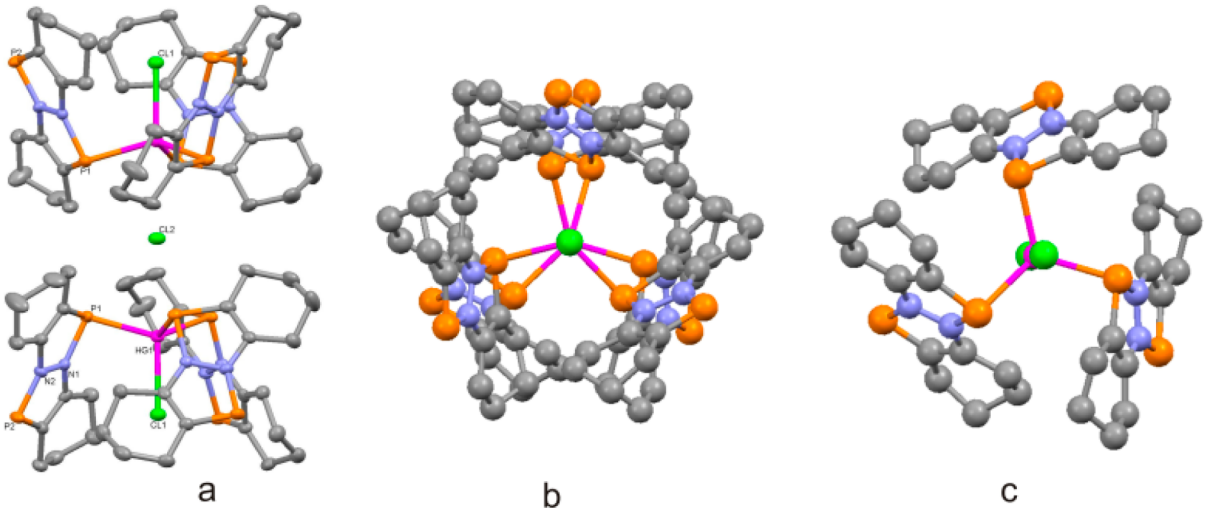

Figure 11. (a) Molecular structure of $[\{(PNNP)_3HgCl\}_2(\mu_6\text{-}Cl)]^+$ (cationic part of **7**). Ellipsoids are drawn at 30% probability. Hydrogen atoms of *c*-hexenyl rings are omitted for clarity. (b) Top view. (c) Top view of the fragment $\{ClHg(PNNP)_3(\mu_6\text{-}Cl)\}$. Selected bond distances (Å) and angles (deg) for **7**: Hg(1)−P(1) 2.560(1), Hg(1)−Cl(1) 2.617(1), P(1)−N(1) 1.768(3), P(1)−C(1) 1.793(3), P(2)−N(2) 1.715(3), P(2)−C(7) 1.744(3), N(1)−C(8) 1.355(4), N(1)−N(2) 1.376(4), N(2)−C(2) 1.392(4), C(1)−C(2) 1.345(5), C(7)−C(8) 1.379(5); P(1)#1−Hg(1)−P(1) 113.12(2), P(1)#1−Hg(1)−Cl(1) 105.52(2), P(1)−Hg(1)−Cl(1) 105.52(2), N(1)−P(1)−C(1) 86.6(2), N(2)−P(2)−C(7) 88.2(2), C(8)−N(1)−N(2) 111.4(3), C(8)−N(1)−P(1) 133.9(2), N(2)−N(1)−P(1) 114.7(2), N(1)−N(2)−C(2) 111.0(3), N(1)−N(2)−P(2) 114.6(2), C(2)−C(1)−P(1) 113.3(3), C(1)−C(2)−N(2) 114.4(3), C(8)−C(7)−P(2) 112.3(2), N(1)−C(8)−C(7) 113.5(3).

The Hg−P bond is expected to dissociate readily in solution because only the ^{31}P NMR signal of the ligand **1** was detected at temperatures ranging from −50 to +50 °C.

In a preliminary paper,[28] Heinicke et al. reported the preparation of the first mercury(II) complex with the σ^2-phosphorus ligand. Note, however, that the ligand described is, in fact, a chelate ligand, and σ^2-phosphorus coordination in this case may be considered to be a result of the rigid geometry because, even in chelate, the Hg−P distance [2.6978(7) Å] is much longer than that observed for complex **7**. Compound **7** so far may be considered the first mercury(II) complex with the "refined" π coordination of the σ^2-phosphorus ligand.

An equivalence of phosphorus atoms in **1** and inclusion of both five-membered heterocycles in the united aromatic system determine an atypical coordination behavior of bisphosphole **1** in comparison with the usual phospholes or phosphines. In the case of N,N′-fused bisphosphole, a novel type of ligand exchange may be realized because coordination of an additional metal ion (M′) onto the second P′ atom weakens the P → M interaction (eq 7).

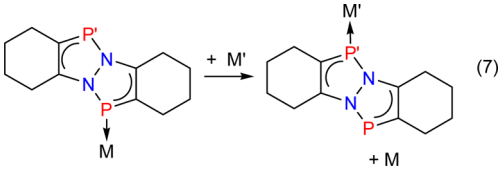

(7)

Such dynamic behavior of the ligand at coordination to the metal ions may affect the crystal structures of the products and the formation of intermolecular and supramolecular associates in solution. So, the adduct of **1** with $SnCl_2$ (**8a** and **8b**), prepared by two methods (eq 8), displays noticeable differences in crystal structure organization and in some physical properties.

The interaction of **1** with $SnCl_2$(diox) results in the formation of adduct **8a**. The molecular structure of **8a** is shown in Figure 12 with selected bond lengths and angles.

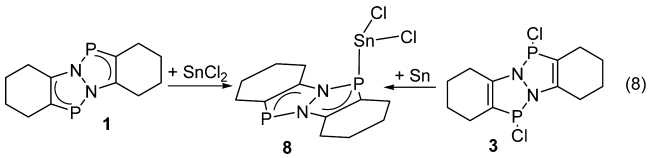

(8)

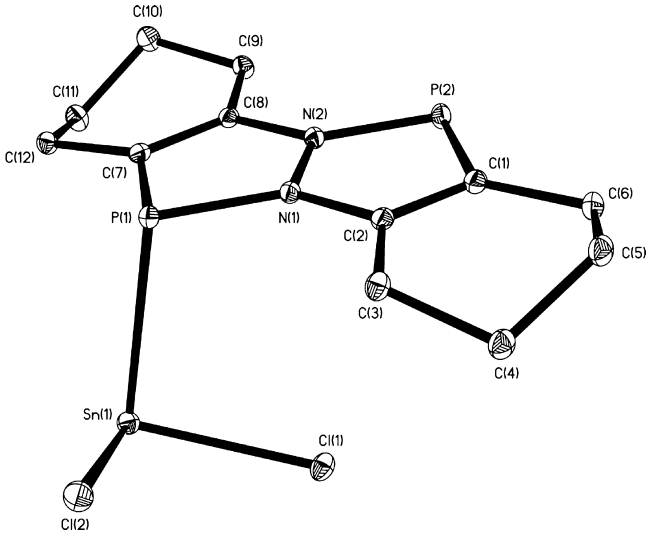

Figure 12. Molecular structure of **8a**. Ellipsoids are drawn at 30% probability. Hydrogen atoms of *c*-hexenyl rings are omitted for clarity. Selected bond distances (Å) and angles (deg) for **8a**: Sn(1)−Cl(2) 2.4893(3), Sn(1)−Cl(1) 2.5231(3), Sn(1)−P(1) 2.7273(3), P(1)−N(1) 1.767(1), P(1)−C(7) 1.797(1), P(2)−N(2) 1.705(1), P(2)−C(1) 1.742(1), N(1)−C(2) 1.357(2), N(1)−N(2) 1.367(1), N(2)−C(8) 1.398(1), C(1)−C(2) 1.384(2), C(7)−C(8) 1.355(2); Cl(2)−Sn(1)−Cl(1) 91.13(1), N(1)−P(1)−C(7) 87.11(5), N(2)−P(2)−C(1) 88.69(5), C(2)−N(1)−N(2) 111.79(9), N(2)−N(1)−P(1) 114.37(7), N(1)−N(2)−C(8) 111.78(9), N(1)−N(2)−P(2) 114.55(7), C(2)−C(1)−P(2) 111.78(9), N(1)−C(2)−C(1) 113.2 (1), C(8)−C(7)−P(1) 112.66(8), C(7)−C(8)−N(2) 114.0(1), C(7)−C(8)−C(9) 127.1(1).

dx.doi.org/10.1021/ic500274h | *Inorg. Chem.* 2014, 53, 3243−3252

Crystal data and some details of the data collection and refinement are given in Table S1 in the SI. To the best of our knowledge, this is the first structurally characterized complex of $SnCl_2$ with a neutral nonchelated phosphine ligand.[29] Stalke and coauthors have shown that a neutral P,N-ligand, diphenyl-(2-picolyl)phosphane, formed a complex with $SnCl_2$ of the structure $[LSnCl]^+[SnCl_3]^-$, demonstrating a P−Sn bond of 2.6962(5) Å in the crystal, whereas the bond between the phosphorus and tin atoms is labile and exists in solution only at lower temperatures.[30]

Coordination to the tin atom causes structural changes in the annulated heterocycles like coordination to the mercury metal center in **7**. The cycle bonded to the tin atom reveals elongation of all chemical bonds relative to the free ligand, whereas the adjacent heterocycle exhibits a decrease in the C−N, P−N, and C−P bond lengths (Table S4 in the SI). The unit cell contains discrete molecules of **8a** with close intermolecular contacts Sn···Cl (3.381−3.534 Å), P···Cl (3.165 Å), and P···P (3.433 Å) (Figure S6 in the SI). The geometry of the P(1) atom is best described as distorted trigonal pyramidal. The Sn−P bond [2.7273(3) Å] forms an angle of 108.7° with the mean plane of a five-membered heterocycle and an angle of 91.0° with the $SnCl_2$ plane.

Alternatively, **8** may be synthesized by the reduction of dichloro derivative **3** with metallic tin. The reaction in THF proceeds quite rapidly to form a red-brown solution. Crystallization from toluene in the presence of metallic tin affords red crystals of **8b**, which differ from **8a** in molecular and crystal structure. The molecular structure of **8b** (Figure S7 in the SI) reveals minor differences in the bond lengths and angles between **8a** and **8b**, which are shown in Table S4 in the SI. Interestingly, the Sn−P bond lengths in **8a** and **8b** are nearly the same as those found in tin(II) compounds containing phosphacyclopentadienide ligands (2.73 and 2.79 Å).[31] The salient feature of the crystal structure is the multiple intermolecular short contacts between the elements, which are shorter or comparable to the sums of the van der Waals radii (Table 2).

Table 2. Intermolecular Close Contacts (Å) and Sums of the van der Waals Radii (in Parentheses) in the Crystal Structure 8b

Sn···Sn	3.66 (4.34)
Sn···P	3.55 (3.97)
Sn···N	3.63 (3.72)
Sn···C(1)	3.57 (3.87)
Sn···C(2)	3.74 (3.87)
P···P	3.66 (3.60)
P···Cl	3.64 (3.60)

The supramolecular organization of **8b** in the crystal is depicted in Figure 13a−c. Among the multiple close contacts, a dimeric structure may be appreciable. The monomers are linked by relatively weak Sn···Sn, Sn···P, Sn···N, and Sn···C interactions (Figure 13b,c). The dimers are based upon the distorted five-coordinate trigonal-bipyramidal geometry at tin. Note, however, that most of the characterized stannylene complexes with additional donor groups bonded to tin involve four-coordinate tin.[32]

The dark-red crystals of **8b** have interesting and unusual properties. They are only stable in contact with a concentrated solution. Washing of the crystals with cold THF (−20 °C) gives a metallic tin of hair-shaped structure and the starting dichloro derivative **3**. Shaking of the ampule leads to the formation of a tin mirror on its wall. Apparently, this reversible transformation is closely related to the supramolecular structure of **8b** because the crystals of **8a** did not show such properties.

Compound **8** demonstrates rather a complicated behavior in solutions assuming the formation of multiple associates. Diluted toluene or THF solutions give no ^{31}P NMR signal (with only a weak singlet from **1**), while concentrated solutions reveal a set of multiplets in the region of 200−230 ppm with small values of $^3J_{P,P}$ (9−20 Hz), which may be the result of P,P′ interaction via the N−N bond. ^{119}Sn NMR spectra did not appear in the concentrated solutions of **8**.

Together with high coordination activity, bis-(diazaphosphole) **1** demonstrates powerful reducing properties. Preliminary studies reveal that **1** easily converts Ph_2PCl to Ph_4P_2 and $PhPCl_2$ to $(PhP)_5$ in hexane at room temperature. The coordination and reducing ability of **1** continue to be investigated in our laboratory and will be described in future reports.

EXPERIMENTAL SECTION

General Remarks. Solvents were purified following standard methods.[33] Toluene and hexane were thoroughly dried and distilled over sodium prior to use. Diethyl ether and THF were dried and distilled over sodium/benzophenone. Tin(II) chloride dioxanate was prepared according to a known method.[34]

Germanium(II) dichloride dioxanate and mercury(II) dichloride were purchased from Sigma-Aldrich Chemical Co. and used as received. All manipulations were performed in a vacuum or under an argon atmosphere using standard Schlenk techniques. NMR spectra were recorded in $CDCl_3$, C_6D_6, or THF-d_8 solutions using Bruker DPX-200 and Bruker AV400 spectrometers. Absorption spectra of **1** and **3** were recorded on a Perkin-Elmer Lambda UV−vis spectrometer. IR spectra were recorded on a Perkin-Elmer 577 device from 4000 to 400 cm^{-1} in Nujol or on a Perkin-Elmer FT-IR spectrometer System 2000 as KBr mulls.

Cyclic Voltammetry. Cyclic voltammograms of **3** have been recorded in *N*,*N*-dimethylformamide (DMF) with a 5×10^{-3} M substrate concentration; Et_4NBF_4 was used as a supporting electrolyte (0.1 mol dm^{-3}) and a glassy carbon electrode as a working electrode (8 mm^2); the reference electrode is a saturated calomel electrode (SCE). Cyclic voltammogram registration was performed with a BASi Epsilon potentiostat (USA). The scan rate was 100 mV s^{-1}. Preparative electrolyses were performed by means of the direct current source B5-49 in a thermostatically controlled cylindrically divided 100 mL electrolyzer (a three-electrode cell). Platinum with a surface area of 20 cm^2 was used as the cathode; a platinum rod was used as the anode. The working electrode potential was determined using the SCE reference electrode. During electrolysis, the electrolyte was stirred with a magnetic stirrer. The saturated solution of Et_4NBF_4 in DMF was used as the anolyte, and the anode compartment was separated by a ceramic membrane.

Computational Details. DFT calculations were performed with the *Gaussian 03* software package (see the SI) at the B3LYP/6-31G(d) level of theory. The optimized geometry of **1** corresponds to energy minima, as indicated by frequency computations. There are no imaginary frequencies in the calculation. For the structure **6** (cationic part) single-point energy calculations were done.

NICS is a technique proposed by Schleyer[21] as an aromaticity index. Following the methodology of Schleyer, we obtained the absolute magnetic shielding at the center of the rings, which is determined by the nonweighted mean of the heavy-atom coordinates.

X-ray Crystallography. The X-ray diffraction data for **1**, **6**, **7**, **8a**, and **8b** were collected on a SMART APEX diffractometer (graphite-monochromated, Mo Kα radiation, ω-scan technique, λ = 0.71073 Å). Structures were solved by direct (**1**, **6**, **8a**, and **8b**) and Patterson (**7**)

dx.doi.org/10.1021/ic500274h | Inorg. Chem. 2014, 53, 3243−3252

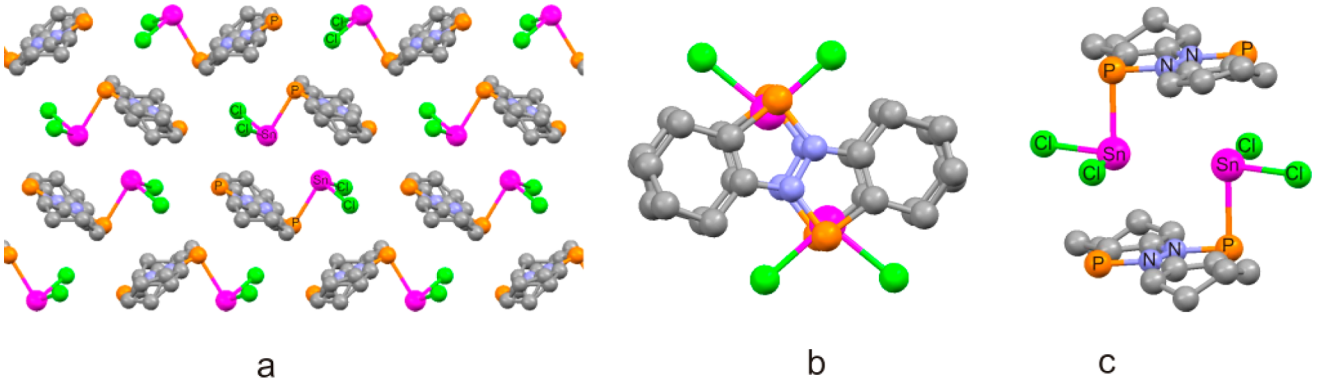

Figure 13. (a) Crystal packing of **8b** showing Sn···Sn, Sn···P, Sn···N, Sn···C, P···P, and P···Cl short contacts. (b) Top view of the dimer in the crystal structure of **8b**. (c) Side view of the dimer in the crystal structure of **8b**.

methods and were refined on F_{hkl}^2 using *SHELXL-97* packages.[35] All non-hydrogen atoms in **1**, **6**, **7**, **8a**, and **8b** were refined anisotropically. All hydrogen atoms were placed in calculated positions and were refined in the riding model. *SADABS*[36] was used to perform absorption corrections in **1**, **6**, **7**, **8a**, and **8b**. The crystal of **7** contains a solvate molecule of THF, which is disordered about an intersection of 2- and 3-fold axes. The solvate molecule of toluene, disposed in a common position, was found in the crystal **8a**. Two carbon atoms of a six-membered carbon cycle in **8b** are disordered over two positions. The main crystallographic data and structure refinement details for **1**, **6**, **7**, **8a**, and **8b** are presented in Table 1. CCDC 947188 (**1**), 947189 (**6**), 947190 (**7**), 947191 (**8a**), and 947192 (**8b**) are given in the SI. These data can also be obtained free of charge at www.ccdc.cam.ac.uk/data_request/cif from the Cambridge Crystallographic Data Centre.

Synthesis. *N,N′-Fused Bisphosphole (**1**).* A solution of **3**[13] (0.32 g, 0.1 mmol) in 25 mL of THF was allowed to react with activated magnesium powder at 20 °C. The reaction began immediately to give a dark-red solution, which soon turned orange. The solution was stirred for 30 min and filtered. The solvent was removed in a vacuum, leaving an orange solid. This solid was recrystallized twice by cooling a concentrated hexane solution at 0 °C. Then **1** was sublimed in vacuo at 110 °C/0.01 mmHg, yielding 0.23 g (92%) of orange needle crystals. Anal. Calcd for $C_{12}H_{16}N_2P_2$: C, 57.60; H, 6.45; N, 11.20; P, 24.76. Found: C, 57.54; H, 6.49; N, 11.25; P, 24.83. ^{1}H NMR (C_6D_6, 295 K): δ 2.79−3.20 (m, 4H, PCCH_2), 2.43−2.72 (m, 4H, NCCH_2), 1.56−2.15 (m, 8H, CCH_2C). ^{13}C NMR: δ 142.8 (d, 2CP, $^1J_{C,P}$ = 48 Hz), 128.6 (m, 2CN), 22.0−25.0 (m, 8CH_2). ^{31}P{^{1}H} NMR: δ 177.0. IR (Nujol, ν/cm^{-1}): 1598m, 1292m, 1271w, 1248m, 1180w, 1153m, 1075w, 1025m, 956m, 884m, 847w, 817m, 788m, 693m, 588w. UV/vis (CH_2Cl_2): λ_{max} = 438.5 nm (ε = 28000 M^{-1} cm^{-1}). MS (ESI): m/z 250 ([M]$^+$), 220 ([M − P]$^+$).

*(**1**$^+$)$_2$(GeCl$_3^-$)$_2$ (**6**).* Germanium dichloride dioxanate (0.232 g, 1.0 mmol) in a THF solution (10 mL) was added to the equimolar mixture of **1** (0.125 g, 0.5 mmol) and **3** (0.161 g, 0.5 mmol) in the same solvent (10 mL). The brown-orange mixture was concentrated up to 3 mL and kept at 0 °C for 1 night. The orange-brown crystals of **6** were separated from the mother liquor, washed with cold THF, and dried in a vacuum. Yield: 0.394 g (92%). Anal. Calcd for $C_{24}H_{32}Cl_6Ge_2N_4P_4$: C, 33.58; H, 3.76; Cl, 24.78. Found: C, 33.52; H, 3.81; Cl, 24.71. ^{1}H NMR (THF-d_8, 295 K): δ 0.7−2.4 (m). IR (Nujol, ν/cm^{-1}): 1346w, 1334w, 1280m, 1241m, 1151w, 1138m, 1068m, 1022m, 958s, 909s, 854m, 811w, 797s, 771w, 724w, 681m, 588m, 551m, 518m, 477w, 477w, 455m.

*[{(**1**)$_3$HgCl}$_2$(μ_6-Cl)]$^+$Cl$^-$ (**7**).* A solution of $HgCl_2$ (90.5 mg, 0.33 mmol) in THF (5.0 mL) was added to a solution of **1** (250.0 mg, 1.0 mmol, 10 mL) in the same solvent. The red mixture was filtered from a metallic mercury dispersion formed as a byproduct, then concentrated up to 3 mL, and kept at 0 °C for 1 week. Red crystals of **7** were separated from the mother liquor, washed with cold THF, and dried in an argon stream. Yield: 88.0 mg (25%). Anal. Calcd for $C_{76}H_{104}Cl_4Hg_2N_{12}OP_{12}$: C, 43.13; H, 4.95; Cl, 6.70; Hg, 18.96. Found: C, 43.09; H, 5.00; Cl, 6.73; Hg, 18.92. ^{1}H NMR (THF-d_8, 295 K): δ 0.9−2.5 (m). ^{31}P NMR: δ 177.0 (widened). IR (Nujol, ν/cm^{-1}): 1278w, 1210w, 1180ww, 1160w, 1126m, 1070m, 1022s, 957w, 909m, 852m, 794s, 680w.

*(**1**)SnCl$_2$(toluene solvate) (**8a**).* A solution of $SnCl_2$(diox) (0.11 g, 0.40 mmol) in THF (5 mL) was added to a solution of **1** (0.10 g, 0.40 mmol) in the same solvent (5.0 mL). THF was removed under reduced pressure. The oily residue was dissolved in 3.0 mL of toluene and kept overnight at 0 °C. The dark-red crystals of **8a** were separated from the mother liquor, washed with cold toluene, and dried under reduced pressure. Yield: 0.17 g (78%). Anal. Calcd for $C_{19}H_{24}Cl_2N_2P_2Sn$: C, 42.90; H, 4.55; Cl, 13.33. Found: C, 42.81; H, 4.60; Cl, 13.28. ^{1}H NMR (toluene-d_8, 295 K): δ 0.7−2.7 (m). ^{31}P NMR: a set of multiplets in the region 200−230 ppm. IR (Nujol, ν/cm^{-1}): IR (Nujol, ν/cm^{-1}): 3027vw, 1602w, 1587m, 1280s, 1250m, 1181w, 1156s, 1123m, 1079m, 1030m, 995w, 909m, 852m, 818m, 732s, wide, 692s, 616w, 589w, 566w, 551w, 493m, 466m.

*(**1**)SnCl$_2$ (**8b**).* A solution of **3** (0.161 g, 0.5 mmol) in THF (5 mL) was added to tin metal turnings (excess) in a vacuum at room temperature. The reaction began immediately and was accompanied by a color change to red-brown. The mixture was slowly stirred for 48 h at 20 °C, and then the solvent was removed under reduced pressure, leaving a red-brown oily product. A small amount of toluene (3.0 mL) was added; the toluene solution was decanted and then kept overnight at 0 °C. The red-brown crystals of **8b** were separated and dried under reduced pressure. Yield: 0.147 g (67%). Anal. Calcd for $C_{12}H_{16}Cl_2N_2P_2Sn$: C, 32.77; H, 3.67; Cl, 16.12. Found: C, 32.82; H, 3.61; Cl, 16.08. ^{1}H NMR (toluene-d_8, 295 K): δ 0.7−2.7 (m). ^{31}P NMR: a set of multiplets in the region 200−230 ppm. IR (Nujol, ν/cm^{-1}): 1587m, 1281s, 1250m, 1183w, 1156s, 1123m, 1083w, 1023m, 995w, 956w, 909m, 852m, 817m, 729 s, wide, 683m, 616w, 589w, 566w, 551w, 494m. The crystals of **8b** decomposed at $t \geq 150$ °C.

■ CONCLUSION

N,N′-Fused bisphosphole **1** prepared by the reduction of the corresponding dichloro precursor **3** displays extraordinary properties compared to the usual azaphospholes. It possesses a much higher coordination activity with metal ions, which is caused by a novel type of complexation. The heteroaromatic 10π-electron system provides two electrons for P → M bond formation, whereas the phosphorus lone pairs are not involved in the coordination. The complexes of **1** with mercury(II) and tin(II) chlorides are supramolecular in nature, containing multiple intermolecular short contacts. The equimolar mixture of **1** and **3** is, in fact, a P−P bridging dimer **5**, which may be detected in diluted nonpolar solvents but dissociates easily in polar solvents. Chloride anion capture by $GeCl_2$(diox) transforms this mixture into salt-like dimer **6** characterized by single-crystal X-ray diffraction. The unusual structure of the

dx.doi.org/10.1021/ic500274h | Inorg. Chem. 2014, 53, 3243−3252

dimer may be explained by the concept of stacked-ring aromaticity assuming a through-space delocalization of π electrons.

■ ASSOCIATED CONTENT

Supporting Information

Crystallographic information for **1**, **6**, **7**, **8a**, and **8b** in CIF format, molecular structure and selected bond lengths and angles for **8b**, ^{13}C NMR spectrum of **1** (sp^2 carbon field), B3LYP/6-31G(d)-calculated structure of **1**, Mulliken charges in dibenzotetraazapenthalene, NBO charges in **1**, and nomenclature of diazaphospholes and related compounds. This material is available free of charge via the Internet at http://pubs.acs.org.

■ AUTHOR INFORMATION

Corresponding Author

*E-mail: akornev@iomc.ras.ru. Phone: +7 (831) 4627795. Fax: +7 (831) 4627497.

Notes

The authors declare no competing financial interest.

■ ACKNOWLEDGMENTS

This work was supported by The Russian President's program "Leading Scientific Schools" (Grant 7065.2010.3) and RFBR Regional Grants 13-03-97096 and 13-03-00891. We thank Dr. O. V. Kouznetsova and N. M. Khamaletdinova for IR measurements and V. Faerman for MS investigation.

■ REFERENCES

(1) Hissler, M.; Lescop, C.; Reau, R. *J. Organomet. Chem.* **2005**, *690*, 2482−2487.

(2) Baumgartner, T.; Reau, R. *Chem. Rev.* **2006**, *106*, 4681−4727.

(3) (a) Albert, I.; Marks, T.; Ratner, M. *J. Am. Chem. Soc.* **1997**, *119*, 6575−6582. (b) Alparone, A.; Reis, H.; Papadopoulos, M. G. *J. Phys. Chem. A* **2006**, *110*, 5909−5918.

(4) (a) Bansal, R. K.; Heinicke, J. *Chem. Rev.* **2001**, *101*, 3549−3578. (b) Schmidpeter, A. In *Comprehensive Heterocyclic Chemistry—II*; Katritzky, A. R., Rees, C. W., Scriven, E. F. V., Eds.; Pergamon: Oxford, U.K., 1996; Vol. *4*, pp 771. (c) Schmidpeter, A. In *Phosphorus−Carbon Heterocyclic Chemistry: The Rise of a New Domain*; Mathey, F., Ed.; Elsevier: Oxford, U.K., 2001; pp 363−461. (d) Schmidpeter, A.; Bansal, R. K.; Karaghiosoff, K.; Steinmüller, F.; Spindler, C. *Phosphorus, Sulfur Silicon Relat. Elem.* **1990**, *49−50*, 349−354. (e) Gupta, N. Recent Advances in the Chemistry of Diazaphospholes. In *Topics in Heterocyclic Chemistry*; Gupta, R. R., Bansal, R. K., Eds.; Springer-Verlag: Berlin, 2010; pp 175−206.

(5) (a) Bansal, R. K. Anellated Azaphospholes. *Topics in Heterocyclic Chemistry*; Springer-Verlag: Berlin, 2008. (b) Bansal, R. K.; Gupta, N.; Gupta, N. *Heteroat. Chem.* **2004**, *15*, 271−287. (c) Gudat, D.; Haghverdi, A.; Hupfer, H.; Nieger, M. *Chem.—Eur. J.* **2000**, *6*, 3414−3425. (d) Nakazva, H. *Adv. Organomet. Chem.* **2004**, *50*, 107−143. (e) Denk, M. K.; Gupta, S.; Ramachandran, R. *Tetrahedron Lett.* **1996**, *37*, 9025−9028. (f) Kraaijkamp, J. G.; Grove, D. M.; van Koten, G.; Schmidpeter, A. *Inorg. Chem.* **1988**, *27*, 2612−2617.

(6) (a) Nyulászi, L.; Veszprémi, T.; Réffy, J.; Burkhardt, B.; Regitz, M. *J. Am. Chem. Soc.* **1992**, *114*, 9080−9084. (b) Nyualszi, L. *Chem. Rev.* **2001**, *101*, 1229−1246.

(7) Chernyak, D.; Gevorgyan, V. *Org. Lett.* **2010**, *12*, 5558−5560.

(8) Xu, H.; Zhang, Y.; Huang, J.; Chen, W. *Org. Lett.* **2010**, *12*, 3704−3707.

(9) Litvinov, I. A.; Karaghiosoff, K.; Schmidpeter, A.; Zabotina, E. Y.; Dianova, E. N. *Heteroat. Chem.* **1991**, *2*, 369−376.

(10) Karaghiosoff, K.; Mahnot, R.; Cleve, C.; Gandhi, N.; Bansal, R. K.; Schmidpeter, A. *Chem. Ber.* **1995**, *128*, 581.

(11) Schmidpeter, A. *Heteroat. Chem.* **1999**, *10*, 529−537.

(12) (a) Altmann, K. L.; Chafin, A. P.; Merwin, L. H.; Wilson, W. S.; Gilardi, R. *J. Org. Chem.* **1998**, *63*, 3352−3356. (b) Carboni, R. A.; Castle, J. E. *J. Am. Chem. Soc.* **1962**, *84*, 2453−2454. (c) Carboni, R. A.; Kauer, J. C.; Castle, J. E.; Simmons, H. E. *J. Am. Chem. Soc.* **1967**, *89*, 2626−2633. (d) Kauer, J. C.; Carboni, R. A. *J. Am. Chem. Soc.* **1967**, *89*, 2633−2637.

(13) Kornev, A. N.; Gorak, O. Y.; Lukoyanova, O. V.; Sushev, V. V.; Panova, J. S.; Baranov, E. V.; Fukin, G. K.; Ketkov, S. Y.; Abakumov, G. A. *Z. Anorg. Allg. Chem.* **2012**, *638*, 1173−1178.

(14) Armbruster, F.; Klingebiel, U.; Noltemeyer, M. *Z. Naturforsch* **2006**, *61b*, 225−236.

(15) Hogel, J.; Schmidpeter, A.; Sheldrick, W. S. *Chem.Ber.* **1983**, *116*, 549.

(16) Batsanov, S. S. *Russ. J. Inorg. Chem.* **1991**, *36*, 1694.

(17) Frisch, M. J.; et al. *Gaussian 03*; Gaussian, Inc.: Pittsburgh, PA, 2003. See the Supporting Information.

(18) The structure calculated for triplet spin multiplicity possesses significantly higher (by 40.1 kcal/mol) total energy and is nonplanar.

(19) (a) Tian, L.; Feiwu, C. *J. Comput. Chem.* **2012**, *33*, 580. (b) Tian, L. *Multiwfn*, version 2.01, http://Multiwfn.codeplex.com.

(20) (a) Bader, R. F. W. Atoms in Molecules. *A Quantum Theory*; Oxford University Press: New York, 1990. (b) Bader, R. F. W. *Acc. Chem. Res.* **1985**, *18*, 9. (c) Bader, R. F. W. *Chem. Rev.* **1991**, *91*, 893.

(21) Schleyer, P. v. R.; Maerker, C.; Dransfield, A.; Jiao, H.; van Eikema Hommes, N. J. R. *J. Am. Chem. Soc.* **1996**, *118*, 6317−6318.

(22) Trofimenko, S. *J. Am. Chem. Soc.* **1966**, *88*, 5588−5592.

(23) Nyulászi, L.; Benkö, Z. Aromatic Phosphorus Heterocycles. *Topics in Heterocyclic Chemistry*; Springer-Verlag: Berlin, 2008; Vol. *6*, pp 27−80.

(24) Sen, S. S.; Khan, S.; Roesky, H. W.; Kratzert, D.; Meindl, K.; Henn, J.; Stalke, D.; Demers, J.-P.; Lange, A. *Angew. Chem., Int. Ed.* **2011**, *50*, 2322−2325.

(25) (a) Wilson, A. J. C. *International Tables for Crystallography*; Kluwer Academic Publishers: London, 1992; Vol. *C*. (b) Bürgi, H.-B.; Dunitz, J. D. *Structure Correlation*; Verlag Chemie: Weinheim, Germany, 1994; Vol. *2*, Appendix A. (c) Dyker, C. A.; Burford, N. *Chem.—Asian J.* **2008**, *3*, 28−36. (d) Burck, S.; Götz, K.; Kaupp, M.; Nieger, M.; Weber, J.; Schmedt auf der Günne, J.; Gudat, D. *J. Am. Chem. Soc.* **2009**, *131*, 10763−10774.

(26) Aihara, J. *J. Phys. Chem. A* **2009**, *113*, 7945−7952.

(27) Le Floch, P. *Coord. Chem. Rev.* **2006**, *250*, 627−681.

(28) Ghalib, M.; Könczöl, L.; Nyulászi, L.; Jones, P. G.; Palm, G. J.; Heinicke, J. W. *Dalton Trans.* **2014**, *43*, 51.

(29) Tin(IV) halides react with tertiary phosphines to form complexes $SnX_4(PR_3)_2$, demonstrating trans configuration of the R_3P ligands. As an example, see: MacDonald, E.; Doyle, L.; Chitnis, S. S.; Werner-Zwanziger, U.; Burford, N.; Deckenc, A. *Chem. Commun.* **2012**, *48*, 7922−7924 and references cited therein.

(30) Objartel, I.; Ott, H.; Stalke, D. *Z. Anorg. Allg. Chem.* **2008**, *634*, 2373−2379.

(31) Westerhausen, M.; Digeser, M. H.; Nolth, H.; Ponikwar, W.; Seifert, T.; Polborn, K. *Inorg. Chem.* **1999**, *38*, 3207−3214.

(32) Petz, W. *Chem. Rev.* **1986**, *86*, 1019−1047.

(33) Perrin, D. D.; Armarego, W. L. F.; Perrin, D. R. *Purification of Laboratory Chemicals*; Pergamon Press: Oxford, U.K., 1980.

(34) Lane, T. J.; McCusker, P. A.; Columba Curran, B. *J. Am. Chem. Soc.* **1942**, *64* (9), 2076−2078.

(35) Sheldrick, G. M. *Acta Crystallogr.* **2008**, *A64*, 112−122.

(36) Sheldrick, G. M. *SADABS v.2.01, Bruker/Siemens Area Detector Absorption Correction Program*; Bruker AXS: Madison, WI, 1998.